Available online at www.sciencedirect.com
SCIENCE DIRECT
Catalysis Today 111 (2006) 280–287
CATALYSIS TODAY
www.elsevier.com/locate/cattod

Phenol hydroxylation using Fe-MCM-41 catalysts

Jung-Sik Choi, Sang-Soon Yoon, Soo-Hyun Jang, Wha-Seung Ahn *

School of Chemical Science and Engineering, Inha University, Incheon 402-751, Republic of Korea

Available online 4 January 2006

Abstract

Highly ordered iron-containing mesoporous material, Fe-MCM-41, with 0.5–4 Fe/Si mol% loading was prepared and characterization was performed using XRD, SEM/TEM, EDS, N_2-sorption, and FT-IR and UV–vis spectroscopies. Fe-MCM-41 exhibited high catalytic activity in phenol hydroxylation using H_2O_2 as oxidant, giving phenol conversion of ca. 60% at 50 °C [phenol:H_2O_2 = 1:1, water solvent]. Effects of Fe contents in Fe-MCM-41 and catalyst concentration, temperature, solvent used, phenol/H_2O_2 mole ratios and H_2O_2 feeding method, and catalyst calcination temperature on conversion profiles were examined. Catalyst recycling was performed to investigate the extent of potential metal leaching. Comparisons in performance were also made using nano-sized Fe_2O_3 particles and Fe-salt impregnated MCM-41 as catalyst. Catechol to hydroquinone in product ratio was close to 2:1 in accordance with a free radical reaction scheme involving Fe^{2+}/Fe^{3+} redox pair and the larger amount of Fe species always achieved the given phenol conversion at a shorter reaction time. As the calcination temperature increases from 400 to 800 °C increasing amount of Fe species came out from the MCM-41 framework. Both tetrahedral Fe and extra-framework Fe species were found catalytically active, but high dispersion of Fe species achieved in Fe-MCM-41 was an advantage.

Keywords: Mesoporous silica; Fe-MCM-41; Phenol hydroxylation; Fe_2O_3 nano-particles

1. Introduction

Dihydroxybenzenes can be synthesized via Rhône–Poulenc process catalyzed by a strong mineral acid [1], or Hamilton system catalyzed by Fenton's reagent [2] in homogeneous systems. These processes have problems with difficulties in continuous operation, separation, and catalyst recovery. Heterogeneous system is more desirable in this regard and Enichem process using TS-1 (titanium silicalite-1) is now commercialized with high hydroquinone selectivity (hydroquinone/catechol ratio = 1) and high hydrogen peroxide efficiency [3,4].

Further investigation is also being made to find more active heterogeneous catalysts than TS-1. Thus transition metal oxide, metal complex and metal ion-exchanged (or supported) on hydrotalcites, resins, and zeolites have been studied by many researchers [5–8]. Sun et al. synthesized Cu–Bi–V–O complex by hydrothermal method and claimed better performance over TS-1 [5]. Zhu et al. and Dubey et al. synthesized hydrotalcites-like compounds by coprecipitation of metal alloys and carried out phenol hydroxylation in varying conditions [6,7].

Fe-containing-molecular sieves are well known active/selective catalysts for oxidation reactions using H_2O_2 or N_2O as oxidant [9]. Dai et al. introduced transition metals in $AlPO_4$-11 and reported that the oxidation activity followed the order of FeAPO-11 > CoAPO-11 > FeMnAPO-11 > MnAPO-11 ≫ $AlPO_4$-11 [10]. Maurya et al. encapsulated Cr(III), Fe(III), Bi(III), Ni(II) and Zn(II) complexes in Y-zeolite, and Fe(III) was shown better performance in phenol hydroxylation than others [11]. Liu and co-workers used 8-qiunolinol–Fe(II) complex immobilized in MCM-41 and concluded that effects of high concentration of active site and reactant in the channels and the distortion of ligand–Fe(II) by pore wall of MCM-41 led to improved activity [12]. Electrophilic attack of hydroxyl radical is proposed to be the reaction pathway for the formation of dihydroxybenzenes over these catalysts. Wang et al. reported that Naβ ion-exchanged with both Fe(II) and Co(II) is very active and selective for phenol hydroxylation at room temperature [13]. A series of iron oxide nano-particles immobilized on a resin was also reported to have high hydroxylation activity due to formation of nano-sized β-FeOOH particles inside resins [8]. Mohamed and Eissa [14]

* Corresponding author. Tel.: +82 32 8607466; fax: +82 32 8720959.
E-mail address: whasahn@inha.ac.kr (W.-S. Ahn).

0920-5861/$ – see front matter © 2005 Elsevier B.V. All rights reserved.
doi:10.1016/j.cattod.2005.10.037

prepared intra-zeolitic Fe(III) as tetrahedral Fe species and other octahedral Fe species prepared by CVD, and claimed that the higher activity of the tetrahedral Fe(III) sample was attributed to the high dispersion of Fe species that are located in framework and to the high crystallinity.

Redox molecular sieves, which are promising for transformations of large organic molecules in liquid phase reactions, had emerged recently by incorporating various transition metal species such as Ti, V, Fe, Zr, Mn, or Sn into the mesoporous silica hosts of M41S type materials [15]. In these materials, large surface areas coupled with uniform mesopores in large pore volume are envisaged to be useful in promoting high dispersion of active sites and in enhancing diffusion rates of reactants/products in liquid phase reactions.

In this work, we have synthesized Fe-MCM-41 in which Fe atoms are incorporated in the framework of MCM-41 by direct-synthesis using transition metal ions introduced in the synthesis gel, and carried out phenol hydroxylation under varying reaction conditions. Reactions were also carried out using Fe salt, Fe_2O_3 nano-particles supported on mesoporous silica, SBA-15 for comparison.

2. Experimental

2.1. Synthesis of catalysts

Fe-containing MCM-41 sample was prepared based on the synthesis recipe of Yuan et al. [16]. The mixture of 0.42 g fumed silica (Cab-Sil M5, Cabot), 29.0 g colloidal silica (Ludox HS-40, 40 wt.%, Dupont) and 4.0 g sodium hydroxide in 18.6 g de-ionized water was added to the mixture of 14.58 g CTMABr (cetyltrimethylammonium bromide, Aldrich) in 72 g de-ionized water. This solution was stirred for 30 min and iron(III) nitrate ($Fe(NO_3)_3{\cdot}9H_2O$, 98%, Aldrich) was added to this solution. The molar ratios of the components in the substrate mixture were SiO_2:Fe_2O_3 = 12.5–100:1, $(CTMA)_2O$:SiO_2 = 0.1:1, OH^-:SiO_2 = 0.5–1:1. Hydrothermal heating was performed at 150 °C for 7 days. The product was washed with copious amount of de-ionized water and dried at 60 °C under vacuum overnight. To remove the templates, the product was subsequently heated at a rate of 2.5 °C min^{-1} to 220 °C holding for 3 h, followed by 1 °C min^{-1} to 550 °C holding for 4 h.

Fe_2O_3 nano-particles of 5 nm average particle size were prepared according to the recipe by Hyeon et al. [17]. 0.2 ml of $Fe(CO)_5$ (1.52 mmol) was added to a mixture containing 10 ml of octyl ether and 1.28 g of oleic acid (4.56 mmol) at 100 °C. The resulting mixture was heated to reflux and kept at that temperature for 1 h. The resulting black solution was cooled to room temperature and 0.34 g of dehydrated $(CH_3)_3NO$ (4.56 mmol) was added. The mixture was then heated to 130 °C under an argon atmosphere and maintained at this temperature, and was slowly increased to reflux and continued for 1 h. The solution was then cooled to room temperature, and ethanol was added to yield a black precipitate, which was then separated by centrifuging. The resulting black powder can be easily re-dispersed in hexane, and the suspended Fe_2O_3 nano-particles were dry-impregnated on pre-calcined mesoporous silica, SBA-15.

Microporous TS-1 (titanium silicalite-1) was prepared following the Enichem patent [18] using TEOS (tetraethyorthosilicate) and Ti *iso*-propoxide with TPAOH (tetrapropylammonium hydroxide, 1 M) as the structure directing agent. TS-1 was synthesized from a substrate having the following composition; SiO_2/TiO_2 = 32.7, TPA^+/SiO_2 = 0.46, H_2O/SiO_2 = 35.

2.2. Characterization

The crystallinity of the samples prepared was measured by X-ray diffraction using Ni-filtered Cu Kα radiation (Philips, PW-1700). The morphology of the samples was examined by TEM (Philips, CM 200). The specific surface area and average pore diameters were determined by N_2 physisorption at liquid nitrogen temperature using a Micromeretics ASAP 2000 automatic analyzer. The surface area was determined by BET method and the pore size distribution was calculated by the Barrett–Joyner–Halenda (BJH) method using the desorption branch of the isotherm. Prior to the measurements, samples were degassed at 100 °C for 1 h and at 350 °C for 4 h at a pressure less than 1.4 Pa. UV–vis diffuse reflectance spectroscopy was performed on a Varian CARY3E double-beam spectrometer using MgO as a reference in the range of 200–750 nm in ambient conditions. FT-IR spectra were recorded in air at room temperature on a Bomem MB104 spectrometer in KBr pellets. Fe contents of the Fe-MCM-41 were measured using SEM–EDS (Kevex/Hitachi S-4200). TGA (Mettler Toledo TGA/SDTA 851) was performed at a heating rate of 5 °C/min up to 800 °C in a flow of air.

2.3. Phenol hydroxylation reaction

Phenol hydroxylation was carried out using Chemistation PPS-2510 fitted with a condenser (Eylela) and gas evolved was measured by a manometer connected to the reactor. In a standard reaction, 0.47 g phenol (C_6H_5OH, 99+%, Aldrich), and 0.03 g Fe-MCM-41 (4 mol%) was added to 15 ml de-ionized water. Hydrogen peroxide (H_2O_2, 35 wt.%, Junsei) was added through a septum to the magnetically stirred phenol solution [phenol to H_2O_2 mol ratio of 1:1] containing catalysts at 50 °C. The change in reaction product was monitored by sampling periodically and analyzed using HP5890 series gas chromatography equipped with a DB-Wax coated capillary column (30 m, 0.32 mm, 0.25 μm) and FID.

3. Results and discussion

3.1. Characterizations of catalysts

Fig. 1a shows the powder XRD pattern of the Fe-MCM-41 (4 mol% Fe). The pattern corresponds to a regular hexagonal channel of MCM-41 structure with a strong (1 0 0) peak followed by three (1 1 0) (2 0 0) and (2 1 1) peaks in the 2θ ranges of 2–7°, which indicates that the mesopore structure of MCM-41 was well preserved even after incorporation of Fe

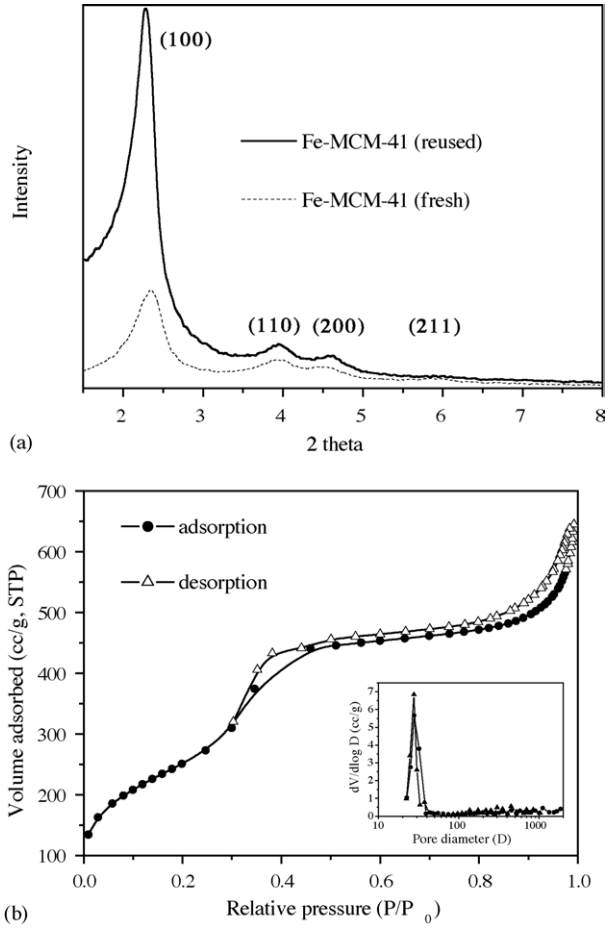

Fig. 1. XRD patterns (a) and N_2 sorption isotherms (b) of Fe-MCM-41.

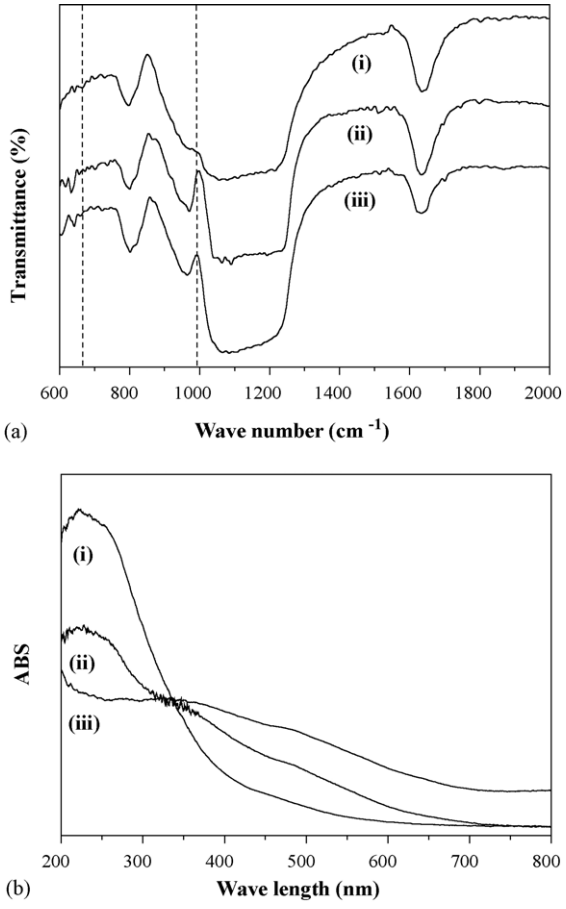

Fig. 3. FT-IR (a) and UV–vis (b) spectra of Fe-MCM-41 (i), FeO_x/MCM-41 (ii), and Fe_2O_3/SBA-15 (iii).

species. The N_2 adsorption isotherm shown in Fig. 1b corresponded to typical type IV adsorption isotherm. Surface area, pore volume, and mean pore diameter were 1189 m^2/g, 1.07 cc/g, and 36 Å, respectively, and exhibited narrow pore size distribution. Fig. 2 corresponds to the TEM images of the material and uniform parallel channels with an ordered pore structure are clearly visible. Fe content in the MCM-41 was measured to be ca. 4 mol% by SEM–EDS analysis, which closely matched the Fe content in the synthesis mixture. Fig. 3a shows FT-IR spectra of Fe-MCM-41 (i), salt impregnated FeO_x/MCM-41 (ii), and Fe_2O_3/SBA-15 (iii). The bands at 660 and 960 cm^{-1} are known to be assignable to Si–O–Fe species [16]. When closely examined, these absorption bands were visible in the Fe-MCM-41 which is incorporated with Fe atoms in the mesoporous silica walls, but no such absorption bands were detected in the other oxide impregnated samples. Fig. 3b compares UV–vis data of the corresponding samples. Fe-MCM-41 (i) shows well defined absorption in the region below

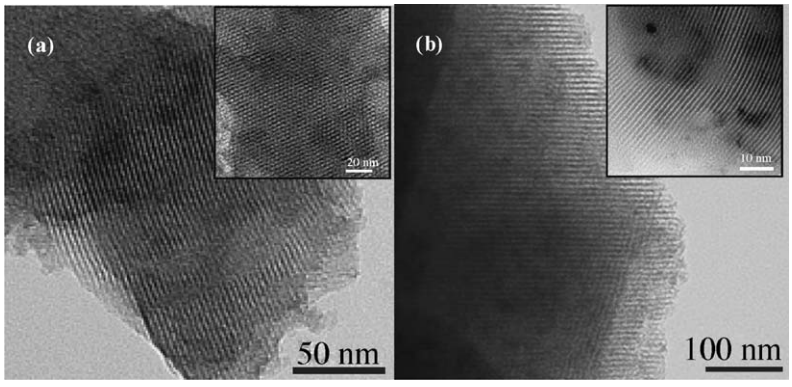

Fig. 2. TEM images of Fe-MCM-41 (a) calcined at 550 °C and (b) at 850 °C.

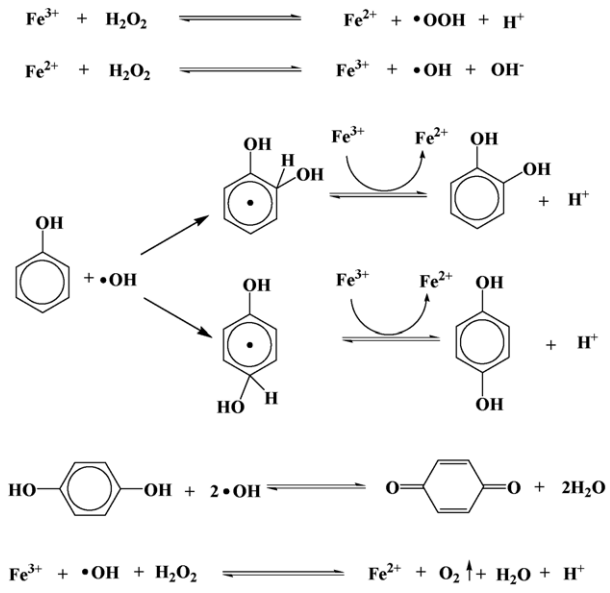

Scheme 1. Phenol hydroxylation reaction pathway of Fe ions [12,14].

440 nm with the strongest peak centered at 245 nm, which indicates uniform oxidation states of Fe species introduced to the MCM-41 framework with Si–O–Fe formation [12]. The other two samples, on the other hand, showed much broader absorption below 800 nm region, which indicates that various kinds of Fe oxidation states coexist in them.

3.2. Phenol hydroxylation reaction

In phenol hydroxylation using Fe-containing catalysts, induction period was usually observed and reaction proceeds mostly during 5–15 min after a short take-off and steadied out to the final state due to depletion of H_2O_2. Phenol conversion under the standard set of experimental condition by Fe-MCM-41 was ca. 60% at 50 °C [phenol:H_2O_2 = 1:1, water solvent]. Catechol, hydroquinone, and black tarry material are formed in liquid phase with gaseous oxygen due to H_2O_2 decomposition. No benzoquinone was detected as in [7,10], which was sometimes reported in small amount by others [12,14].

Phenol hydroxylation has been known to proceed via a redox mechanism involving Fe(III)/Fe(II) redox pair as described in Scheme 1, and the ability of the framework transition metal in zeolytic materials to change oxidation states between (II) and (III) is well-known [10].

H_2O_2 alone without phenol at the standard reaction condition decomposed to oxygen with Fe(II) or Fe(III) salts (ca. 30%) but no detectable H_2O_2 decomposition took place with Fe-MCM-41(<3%) indicating that Bronsted acidity which can cause H_2O_2 decomposition is negligible in Fe-MCM-41. Fe species in the MCM-41 framework seem to require more energy than that of Fe ions to generate OH radicals from H_2O_2 and the phenol hydroxylation proceeded more slowly with an induction period, whereas no induction period was observed with Fe(II) or Fe(III) salts.

Effects of various reaction parameters on phenol hydroxylation were studied and the experimental findings were interpreted based on the redox mechanism proposed. Phenol hydroxylation was also conducted using other Fe-containing catalysts prepared by different procedures but at the same level of Fe content (4 mol%).

3.2.1. Effect of reaction temperature

As shown in Fig. 4, more pronounced induction period was observed at lower reaction temperatures, and the total reaction time became significantly shortened from 150 to 10 min with increases in the reaction temperature from 20 to 70 °C. Final phenol conversion decreased slightly with decreases in reaction temperature. At temperature below 10 °C, final phenol conversion decreased to 42% because of phenol solubility limit in water. Above 80 °C, conversion of phenol also decreased due to enhanced H_2O_2 decomposition as detected by increases in the volume of gaseous product. Similar observation was reported for other Fe-containing catalysts [7,12]. This result suggests that the redox transition of Fe(III)/Fe(II) pair in MCM-41 is in operation even at room temperature. This fast reaction is in contrast to TS-1, which has optimal reaction temperature in the range of 60–90 °C accompanied by longer reaction time, with the phenol conversion being very sensitive to the reaction temperature.

3.2.2. Effect of solvents

As shown in Fig. 5, conversion of phenol was strongly dependent on the solvent used. Phenol conversion was ca. 60% in water and ca. 20% in acetonitrile. Phenol hydroxylation virtually did not proceed in acetone or in ethanol (less than ca. 4%). In water, both phenol and H_2O_2 dissolved easily and active hydroxyl radicals can be formed effectively upon contact with Fe sites. This effect of the solvents strongly supports that radical reaction mechanism is in operation in phenol hydroxylation. Radicals generated are more stable in polar solvents, and the polarity order of the solvents is water > acetonitrile > acetone and ethanol, which was exactly the same order as in phenol

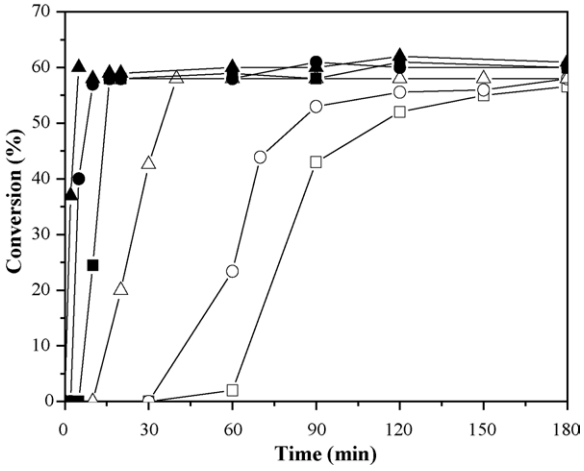

Fig. 4. Effect of reaction temperature on phenol conversions in water over Fe-MCM-41 (4 mol%) calcined at 550 °C with phenol:H_2O_2 ratio of 1:1; (□) 20 °C, (○) 30 °C, (△) 40 °C, (■) 50 °C, (●) 60 °C and (▲) 70 °C.

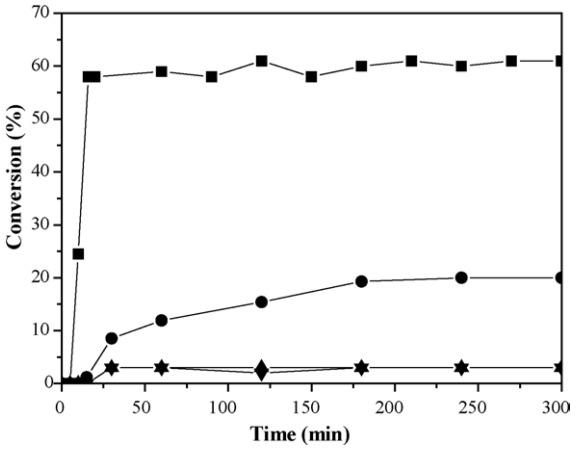

Fig. 5. Effect of solvents on phenol conversions at 50 °C over Fe-MCM-41 (4 mol%) calcined at 550 °C with phenol:H_2O_2 ratio of 1:1; (■) water, (●) acetonitrile, (▲) acetone and (▼) ethanol.

conversions obtained in this study. Ethanol is also a well-known scavenger of hydroxyl radical, and negligible reaction took place.

3.2.3. Effect of phenol/H_2O_2 ratio and oxidant feeding method

Reaction was carried out with varying amount of H_2O_2 to a fixed amount of phenol in 1:1 to 1:0.33 (phenol:H_2O_2) ratios. As shown in Fig. 6a, phenol conversion increased and induction period became shorter with increases in the amount of H_2O_2 injected. At the standard reaction condition (phenol:H_2O_2 ratio of 1:1), ca. 60% of phenol conversion was obtained and among which effective conversion to dihydroxybenzenes amounted to ca. 38%. Hydroquinone to catechol ratio remained close to 1:2 in all cases. As H_2O_2 was reduced to 1/3 (phenol:H_2O_2 ratio 1:0.33), conversion decreased to 41%, and it was more H_2O_2 efficient to run the reaction at the lower H_2O_2 to phenol ratios: H_2O_2 efficiency based on the amount of catechol and hydroquinone formed was 38, 41, and 45%, respectively, as the phenol to H_2O_2 ratio varied from 1:1 to 1:0.33, which was significantly higher than the one reported by Han et al. [19]. The effect of H_2O_2 injection scheme was also examined at phenol to H_2O_2 ratio of 1:2. As shown in Fig. 6b, the corresponding phenol conversion with double injection with two equal portions was better (89%) than that with one injection scheme (80%). Apparently, excess amount of H_2O_2 in phenol hydroxylation using Fe-MCM-41 is undesirable due to competing H_2O_2 decomposition, which can be circumvented by multiple feeding of the oxidant and keeping H_2O_2 to phenol ratios low.

3.2.4. Effect of catalyst calcination temperature

Fe-MCM-41 catalyst was treated at different calcination temperatures before reaction. As shown in the UV–vis spectra in Fig. 7a, the portion of the absorption band of the material near 345 nm progressively grew in magnitude and the spectra shifted to longer wavelength region as the calcination temperature increases. Even at 550 °C which is normally employed to remove the surfactant molecules inside mesopores, UV–vis spectra indicated the formation of extra-framework oxidized Fe species. Spectral shift to longer wavelength region accompanied by a wide absorption tails becomes more pronounced as calcination temperature increases to 750 and 850 °C. According to the corresponding XRD patterns of the materials, intensity of (1 0 0) steadily decreased with increasing calcination temperature and (1 1 0) and (2 0 0) minor peaks disappeared at 750 °C. At 850 °C, even partial collapse of MCM-41 structure was implicated. These results point out that Fe species become aggregated and the resulting cluster becomes bigger as calcination temperature increases. TEM analysis in Fig. 2c clearly shows the Fe cluster formed at 850 °C. Corresponding phenol conversions were found to be 61, 58, 55, and 12% for those calcined catalyst at 550, 650, 750, and 850 °C as shown in Fig. 8. No reaction took place without calcination, which indicates that few active Fe-sites on the external surface exist in Fe-MCM-41. The catalyst calcined at excessively high temperature has shown low catalytic activity due to bad dispersion of the active Fe sites and changes to higher oxidation state of the Fe species, which would reduce the unsaturated coordination numbers and make transition between Fe(II) and Fe(III) oxidation states difficult [8].

3.2.5. Effect of Fe contents in Fe-MCM-41

Fe-MCM-41 catalysts were prepared with varying amount of Fe from 1 to 4 mol% Fe/Si in the substrate mixture, and

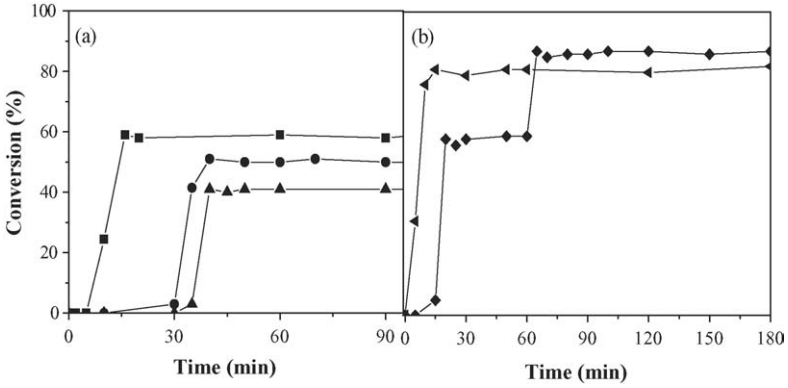

Fig. 6. Effect of phenol to H_2O_2 ratio at 50 °C in water over Fe-MCM-41 (4 mol%) calcined at 550 °C (a); (■) 1:1, (●) 1:0.66, (▲) 1:0.33 (Phenol:H_2O_2), and injection scheme (b); (◆) H_2O_2 injection in two portions, (▼) H_2O_2 injection in 1 portion (Phenol:H_2O_2 = 1:2).

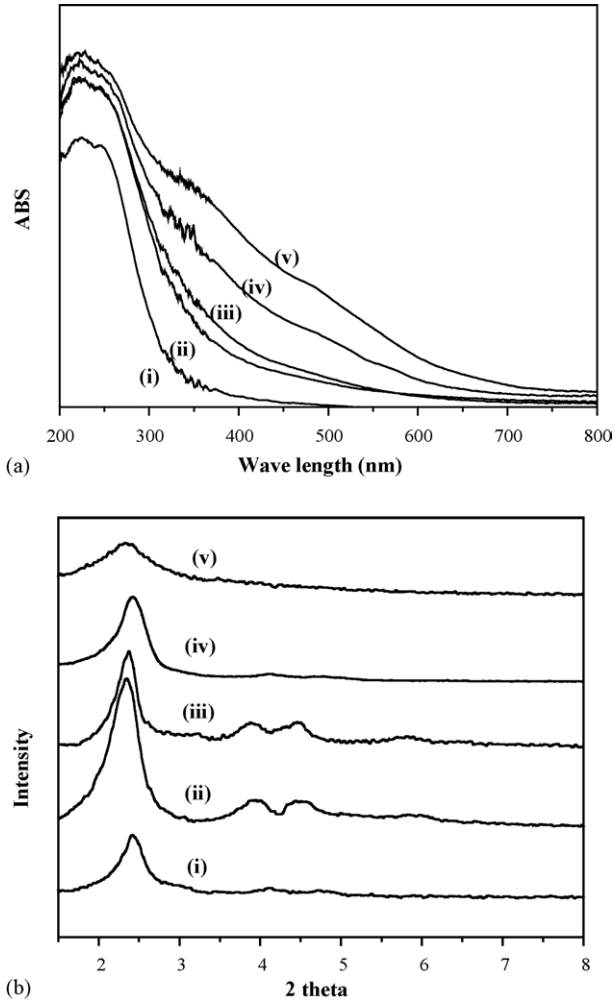

Fig. 7. UV–vis spectra (a) and XRD patterns (b) of Fe-MCM-41: (i) before calcination, (ii) calcined at 550 °C, (iii) 650 °C, (iv) 750 °C and (v) 850 °C.

SEM–EDS analysis showed that virtually all the Fe species in the synthesis gel were incorporated to the corresponding solid catalysts. XRD patterns were identical and UV–vis spectra of the catalysts were also almost the same but with slight differences in the absorption band at 220–350 nm corresponding to the tetrahedral and octahedral Fe species (not shown); both absorbance near 220 nm and at 350 nm decreased as Fe content in Fe-MCM-41 decreased. This is in accordance with the expectation that smaller amount of Fe species in synthesis batch would lead to the better formation of tetrahedral Fe species in the framework. Corresponding reaction profiles are shown in Fig. 9 using 30 mg catalyst each. Induction period increased from 15, 60, and to 120 min and total reaction time lengthened from 45, 120, and to 150 min for Fe contents of 3, 2, and 1 mol%. Reaction was also carried out using the different amount of Fe-MCM-41 (4 mol%) from 5, 10, 30, 50, and 100 mg. Induction period steadily decreased with the increasing amount of catalyst and the reaction virtually took off immediately with 100 mg catalyst. Phenol conversion concurrently increased from 53 to 62% but remained virtually the same above 30 mg catalyst. Induction period was found strongly dependent on the amount of Fe species but total conversion was insensitive to it. Since it takes longer to generate sufficient OH radicals to initiate the reaction with phenol with smaller number of active sites, and longer induction period is observed. Active Fe(III) sites are involved again in the formation of final dihydroxybenzenes, and consequently smaller number of Fe(III) sites result in slow reaction rate after induction period.

3.2.6. Catalyst recycling

Catalyst-recycling test was conducted to have a measure of metal leaching. Used catalyst was separated by filtration and washed with copious amount of water and acetone followed by calcination at 550 °C. As shown in Fig. 10, first reaction cycle was terminated after 10 min with 5 min induction period and 60% of phenol conversion was achieved. In the second reaction using the regenerated catalyst, induction period of ca. 60 min was observed with 90 min reaction time and conversion dropped to 56%. The third reaction showed the same trend as in the second reaction with 55% of phenol conversion. According

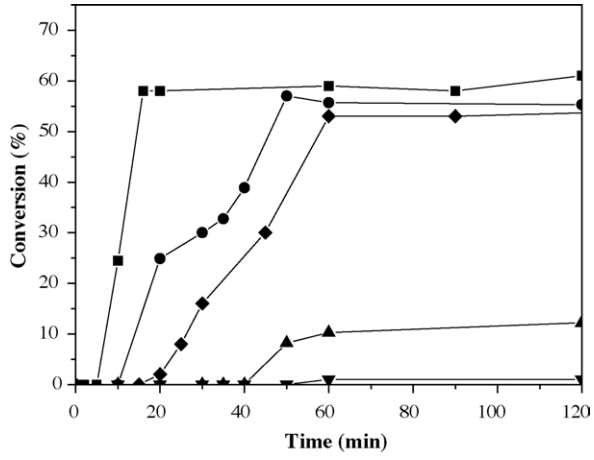

Fig. 8. Phenol conversion profiles at 50 °C and phenol:H_2O_2 = 1:1 in water using Fe-MCM-41 (4 mol%) calcined at various temperatures; (■) 550 °C, (●) 650 °C, (◆) 750 °C, (▲) 850 °C and (▼) no calcination.

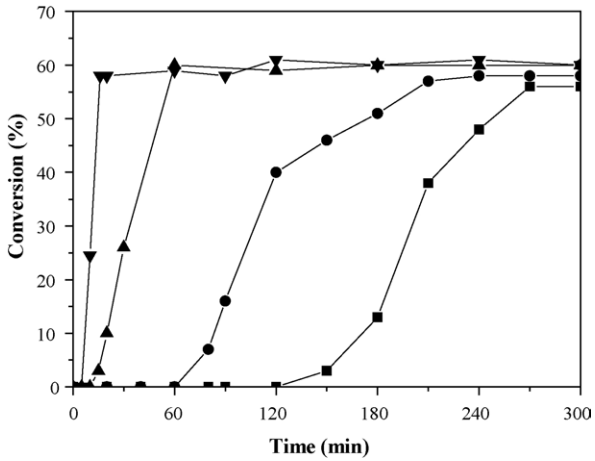

Fig. 9. Phenol conversions at 50 °C and phenol:H_2O_2 = 1:1 in water over Fe-MCM-41 calcined at 550 °C with different Fe contents; (▼) 4 mol%, (▲) 3 mol%, (●) 2 mol% and (■) 1 mol%.

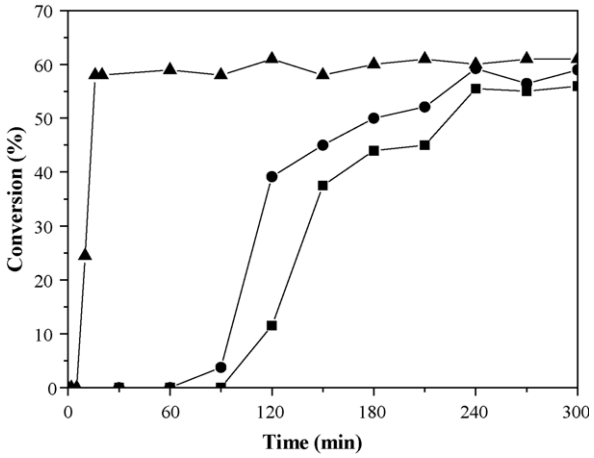

Fig. 10. Catalyst recycling effect on the phenol conversions at 50 °C and phenol:H_2O_2 = 1:1 in water over Fe-MCM-41 calcined at 550 °C; (▲) first cycle (4 mol%), (●) second cycle (2.8 mol%), (■) third cycle (2.5 mol%) (Fe/Si measured by SEM–EDS).

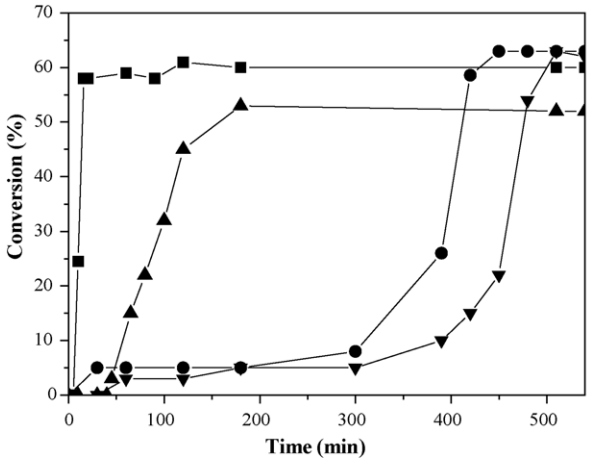

Fig. 11. Comparison of phenol conversion profiles obtained at 50 °C and phenol:H_2O_2 = 1:1 in water using different Fe-containing catalysts; (■) Fe-MCM-41, (▲) FeO_x/MCM-41, (●) Fe_2O_3-NPs and (▼) Fe-NPs/SBA-15.

to SEM–EDS analysis, Fe contents of these catalysts decreased from 4 to 2.8 and then 2.5%. It seems the catalyst becomes stable after 2–3 runs. Phenol conversion in the first reaction was believed to be somewhat higher due to extra-framework Fe clusters contributing to the radical reaction (vide infra). According to the reaction Scheme 1, H^+ is predicted to form during the reaction and indeed pH of the reaction medium showed significant drop in pH from 6.0 to 2.7 at the end of reaction. It can be conjectured that under this acidic condition Fe clusters of extra-framework is partly removed but framework Fe species remained more or less conserved in the second and third run. Interestingly, XRD intensity of the reused catalyst increased significantly as shown Fig. 1. It seems hydrothermal restructuring of the MCM-41 host material [20] accompanied by the removal of the extra-framework Fe clusters is the reason for the enhanced crystallinity of Fe-MCM-41.

3.2.7. Comparison of performances with other catalysts

Table 1 shows the performance of other Fe-containing catalysts for phenol hydroxylation reaction and Fig. 11 shows the reaction profiles for selected catalysts of Fe-MCM-41, FeO_x/MCM-41 (Fe-salt impregnated on MCM-41), Fe-NPs (Fe_2O_3 nano-particles), and Fe_2O_3/SBA-15 (Fe-NPs impregnated on SBA-15). As mentioned earlier, $Fe(NO_3)_3$ salt was highly soluble in aqueous solution and very active with reaction time less than 5 min with 70% phenol conversion. However, effective conversion to dihydroxybenzene was only 29% and large amount of tar was formed. FeO_x/MCM-41 is believed to be made of mostly extra-framework Fe oxides and phenol conversion was lower than Fe-MCM-41 with longer reaction time, which indicates that octahedral extra-framework Fe species are less active than tetrahedrally coordinated ones as reported earlier [14,21]. Fe-NPs showed comparable performance to Fe-MCM-41 but excessively long induction period was observed. Fe-NPs are made of ca. 5 nm Fe_2O_3 particles but TG/DTA analysis showed that they are covered with a surfactant layer of 29% to prevent aggregation between Fe-NPs. Apparently, H_2O_2 has to pass through this surfactant layer in order to approach the active sites on Fe-NPs. Hindered mass transfer of reactants was more pronounced in Fe_2O_3/SBA-15 and even longer induction period was observed accompanied by drop in conversion.

TS-1 does not show induction period and reaction proceeded steadily in a continuous manner indicating different reaction mechanism is prevailing. Phenol conversion was 45% with effective conversion to dihydroxybenzenes to 28%. However, more industrially demanding hydroquinone selectivity was higher than Fe-containing catalysts with catechol to hydroquinone ratio of 1:4.

Table 1
Catalytic activities of various catalysts in phenol hydroxylation

Samples	Time (min)	Conversion (%)		Product selectivity (%)	
		X_{Phenol}	X_{CAT+HQ}	CAT	HQ
Fe-MCM-41	10	60	38	68	32
$Fe(NO_3)_3$	<5	70	29	69	31
FeO_x/MCM-41	50	52	34	72	28
Fe-NPs	450	63	36	72	28
Fe-NPs/SBA-15	510	57	28	73	27
TS-1[a]	1200	45	28	58	42

[a] Reaction condition: temperature 70 °C, solvent acetonitrile.

4. Conclusions

High quality Fe-MCM-41 with up to 4 mol% Fe content could be prepared. Fe in MCM-41 framework was not stable enough above 750 °C calcination and some came out from the silica framework. Fe-MCM-41 was found effective as catalyst in phenol hydroxylation. Catechol to hydroquinone in product ratio was close to 2:1 in accordance with a free radical reaction scheme involving Fe(III)/Fe(II) redox pair. Higher amount of Fe species always achieved the given phenol conversion at a shorter reaction time. Comparison with the performance of other Fe-containing catalysts such as Fe-salt impregnated MCM-41 or Fe_2O_3 nano-particles showed that higher level of

dispersion achieved in Fe-MCM-41 through the formation of Fe–O–Si bond in the mesoporous material is an advantage for phenol hydroxylation.

Acknowledgement

This work was supported by grant No. R01-2003-000-10382-0 from the Basic Research Program of the Korea Science & Engineering Foundation.

References

[1] F. Bourdin, M. Costantini, M. Jouffret, G. Latignan, German Patent 2,064,497 (1971).
[2] G.A. Hamilton, J.P. Friedman, P.M. Campbell, J. Am. Chem. Soc. 88 (1966) 5266.
[3] A. Esposito, M. Taramasso, C. Neri, F. Buonomo, British Patent 2,116,974 (1985).
[4] J.A. Martens, P.H. Buskens, P.A. Jacobs, A. van der Pol, J.H.C. van Hooff, C. Ferrini, H.W. Kouwenhoven, P.J. Kooyman, H. van Bekkum, Appl. Catal. A: Gen. 99 (1993) 71.
[5] J. Sun, X. Meng, Y. Shi, R. Wang, S. Feng, D. Jiang, R. Xu, F.S. Xiao, J. Catal. 193 (2000) 199.
[6] K. Zhu, C. Liu, X. Ye, Y. Wu, Appl. Catal. A: Gen. 168 (1998) 365.
[7] A. Dubey, V. Rives, S. Kannan, J. Mol. Catal. A: Chem. 181 (2002) 151.
[8] D. Wang, Z. Liu, F. Liu, X. Ai, X. Zhang, Y. Cao, J. Yu, T. Wu, Y. Bai, T. Li, X. Tang, Appl. Catal. A: Gen. 174 (1998) 25.
[9] A. Ribera, I.W.C.E. Arends, S. de Vries, J. Perez-Ramirez, R.A. Sheldon, J. Catal. 195 (2000) 287.
[10] P.-S.E. Dai, R.H. Petty, C.W. Ingram, R. Szostak, Appl. Catal. A: Gen. 143 (1996) 101.
[11] M.R. Maurya, S.J.J. Titinchi, S. Chand, I.M. Mishra, J. Mol. Catal. A: Chem. 180 (2002) 201.
[12] C. Liu, Y. Shan, X. Yang, X. Ye, Y. Wu, J. Catal. 168 (1997) 35.
[13] J. Wang, J.N. Park, X.Y. Wei, C.W. Lee, Chem. Commun. (2003) 628.
[14] M.M. Mohamed, N.A. Eissa, Mater. Res. Bull. 38 (2003) 1993.
[15] I.W.C.E. Arends, R.A. Sheldon, M. Wallau, U. Schuchardt, Angew. Chem. Int. Ed. 36 (1997) 1144.
[16] Z.Y. Yuan, S.Q. Liu, T.H. Chen, J.Z. Wang, H.X. Li, J. Chem. Soc. Chem. Commun. (1995) 973.
[17] T.H. Hyeon, S.S. Lee, J.N. Park, Y.H. Chung, H.B. Na, J. Am. Chem. Soc. 123 (2001) 12798.
[18] M. Taramasso, G. Perego, B. Notari, US Patent 4,410,501 (1983).
[19] Y. Han, X. Meng, H. Guan, Y. Yu, L. Zhao, X. Xu, X. Yang, S. Wu, N. Li, F. Xiao, Microporous Mesoporous Mater. 57 (2003) 191.
[20] M. Kruk, M. Jaroniec, A. Sayari, Microporous Mesoporous Mater. 27 (1999) 217.
[21] S. Bordiga, R. Buzzoni, F. Geobaldo, C. Lamberti, E. Giamello, A. Zecchina, G. Leofanti, G. Petrini, G. Tozzola, G. Vlaic, J. Catal. 158 (1996) 486.